CHEMISTRY
A European Journal

A Journal of
ChemPubSoc Europe

## Accepted Article

**Title:** [Ru(dcbpy)2dppz]2+/Fullerene Co-Sensitized PTB7-Th for Ultrasensitive Photoelectrochemical MicroRNA Assay

**Authors:** Lingying Xia, Yingning Zheng, Wenbin Liang, Mengjie Li, Tao Hu, Ruo Yuan, and Yaqin Chai



**To be cited as:** *Chem. Eur. J.* 10.1002/chem.201806005

**Link to VoR:** http://dx.doi.org/10.1002/chem.201806005

Supported by
ACES

WILEY-VCH

# $[Ru(dcbpy)_2dppz]^{2+}$/Fullerene Co-Sensitized PTB7-Th for Ultrasensitive Photoelectrochemical MicroRNA Assay

Ling-Ying Xia, Ying-Ning Zheng, Wen-Bin Liang, Meng-Jie Li, Tao Hu, Ruo Yuan*, Ya-Qin Chai*

*Key Laboratory of Luminescent and Real-Time Analytical Chemistry (Southwest University), Ministry of Education, College of Chemistry and Chemical Engineering, Southwest University, Chongqing 400715, PR China*

**Abstract:**

Here, a novel co-sensitization photoelectrochemical (PEC) strategy was established using donor-acceptor-type photoactive material poly{4,8-bis[5-(2-ethylhexyl)thiophen-2-yl]benzo[1,2-b:4,5-b′]dithiophene-2,6-diyl-alt-3-fluoro-2-[(2-ethylhexyl)carbonyl] Thieno[3,4-b]thiophene-4,6-diyl} (PTB7-Th) as signal indicator, which was co-sensitized by bis(4,4′dicarboxyl-2,2′-bipyridyl)(4,5,9,14-tetraaza-benzo[b]triphenylene)ruthenium(II) ($[Ru(dcbpy)_2dppz]^{2+}$) embedded in the grooves of DNA duplex and fullerene (nano-$C_{60}$) immobilized on the surface of DNA nanoflowers (NFs) for microRNA assay. $[Ru(dcbpy)_2dppz]^{2+}$ and nano-$C_{60}$ could effectively enhance the photoelectric conversion efficiency (PCE) of PTB7-Th attributing from the well-matched energy levels among nano-$C_{60}$, $[Ru(dcbpy)_2dppz]^{2+}$ and PTB7-Th, leading to an obviously enhanced photocurrent signal. Meanwhile, a target-recycling magnification technique based on duplex-specific nuclease (DSN) was applied in this work for obtaining higher detection sensitivity. Our proposed biosensor demonstrated excellent analytical properties within a detection linear range of 2.5 fM to 2.5 nM and a limit of detection down to 0.83 fM. Impressively, this co-sensitization PEC strategy offers an effective and convenient avenue to significantly

[1] *Corresponding authors at: Tel.: +86 23 68252277, fax: +86 23 68253172.
E-mail addresses: yuanruo@swu.edu.cn (R. Yuan); yqchai@swu.edu.cn (Y. Q. Chai).

improve PCE of photoactive material, resulting in a remarkably improved photocurrent signal for ultrasensitive and highly accurate detection of various targets.

*Keywords:* Co-sensitization; PTB7-Th; $[Ru(dcbpy)_2dppz]^{2+}$; Nano-$C_{60}$

## 1. Introduction

Photoelectrochemical (PEC) strategy as a potential assay method has received increasing research interests in analytical fields due to its intrinsic advantages over traditional assay, such as higher sensitivity, easier operation procedures, and lower background signal.[1-5] Poly{4,8-bis[5-(2-ethylhexyl)thiophen-2-yl]benzo[1,2-b:4,5-b′] dithiophene-2,6-diyl-alt-3-fluoro-2-[(2-ethylhexyl)carbonyl]Thieno[3,4-b]thio-phene-4,6-diyl} (PTB7-Th) as a donor-acceptor type photoelectric material has been widely applied in PEC biosensor owing to its merits of well film-forming property, excellent chemical stability and easy operation procedure, which could produce stable PEC signal without any addition of electron donor or acceptor.[6-8] Considering the photogenerated signal of PTB7-Th was limited by its restricted photoelectric conversion efficiency (PCE), lots of efforts have been made to improve the PCE of PTB7-Th. For example, our group fabricated a PEC biosensor using polyethylene glycol as a nanocapsule packaged PTB7-Th and its sensitizer to improve the PCE of PTB7-Th.[9] Lately, our group reported a PEC biosensor using polyaniline, fullerene (nano-$C_{60}$) and perylenetetracarboxyl diimide as the sensitizers of PTB7-Th, achieving the cascade amplification of PTB7-Th PCE.[10] Despite the PCE of PTB7-Th was improved through constructing different sensitization structures based on PTB7-Th, the preparation process of sensitizers was complex and time-consuming. Therefore, it is highly needful to establish a simple and effective sensitized strategy to enhance the PCE of PTB7-Th and construct an ultrasensitive biosensor for PEC assay.

Ruthenium(II) polypyridyl complexes as traditional type photosensitive materials, have received special attentions owing to their wide range applications including organic light-emitting devices,[11,12] dye-sensitized solar cells [13,14] and photoinduced hydrogen generation[15] in the past few decades taking into account of their advantages in chemical stability and well-characterized photophysical properties.[16] Bis(4,4′dicarboxyl-2,2′-bipyridyl)(4,5,9,14-tetraazabenzo[b]triphenylene)ruthenium(II) ($[Ru(dcbpy)_2dppz]^{2+}$) as a sort of the derivatives of Ru(II) polypyridyl complexes, could be embedded into DNA duplex because of its high binding affinity with DNA duplex structure and showed a fast electron transformation ability when it was embedded into DNA duplex.[17-20] Meanwhile, nano-$C_{60}$ as another conventional type sensitizer with rich $\pi$ electrons could be immobilized on the surface of DNA duplex assisted with $\pi$-$\pi$ conjunction.[21,22] More importantly, the energy band gaps matched well among nano-$C_{60}$ (2.6 eV), $[Ru(dcbpy)_2dppz]^{2+}$ (2.36 eV, the calculation process was showed in Supporting Information) and PTB7-Th (1.58 eV), which made it possible to significantly improve the PCE of PTB7-Th and increase the photocurrent.[23-25] Considering those advantages, we used $[Ru(dcbpy)_2dppz]^{2+}$ and nano-$C_{60}$ as feasible sensitizers for PTB7-Th in this work. For the purpose of increasing the immobilization amount of sensitizers on the surface of PTB7-Th, DNA nanoflowers (DNA NFs) with numerous DNA duplex were employed as an excellent immobilization platform because $[Ru(dcbpy)_2dppz]^{2+}$ and nano-$C_{60}$ could be numerously embedded in the grooves of DNA duplex and immobilized on the surface of DNA NFs, respectively.[26,27] Through such a simple and effective proposal, a co-sensitization structure of nano-$C_{60}$/$[Ru(dcbpy)_2dppz]^{2+}$/PTB7-Th was presented, which is expected to increase the PCE of PTB7-Th.

This work has proposed an ultrasensitive PEC assay based on a donor-acceptor-type photoactive material PTB7-Th as signal indicator, which was co-sensitized by $[Ru(dcbpy)_2dppz]^{2+}$ and nano-$C_{60}$ to obtain an obviously enhanced photocurrent signal, achieving the assay of microRNA with the assistance of duplex-specific nuclease (DSN)[28] assisted target-recycling magnification technique. As shown in Scheme 1, an initial photocurrent signal was obtained by filming PTB7-Th on bare glassy carbon electrode (GCE). In the presence of target microRNA-141, the target was transduced to product DNA *via* a DSN assisted target-recycling magnification technique. The product DNA could trigger a rolling circle repetition (RCR) [29-32] reaction, leading to the generation of DNA NFs with considerable DNA duplex structure on the surface of GCE. And then, $[Ru(dcbpy)_2dppz]^{2+}$ was numerously immobilized through intercalation in the grooves of DNA duplex, resulting in a significantly signal enhancement. Moreover, nano-$C_{60}$ as another conventional type sensitizer could be immobilized on the surface of DNA NFs by $\pi$-$\pi$ conjunction, providing a further enhancement of photocurrent response. The increased photocurrent response is positively interrelated with the increasing target concentration with microRNA-141 as a model, achieving the quantitative assay for microRNA-141. As far as we know, the specific expression of microRNA is related with the occurrence of tumor. This study proposed a new co-sensitization strategy for ultrasensitive and highly selective assay of microRNA, exhibiting great potential in PEC assay and promising application for cancer diagnosis.

10.1002/chem.201806005

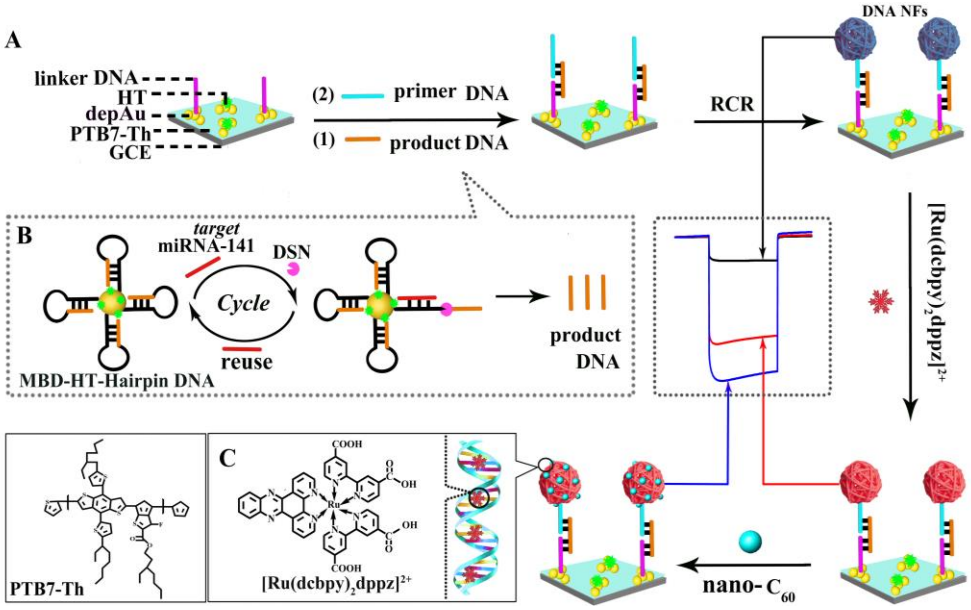


**Scheme 1.** Schematic illustration of (A) Target-Recycling Magnification Based on DSN; (B) Biosensor Assembling Process; (C) Intercalation of $[Ru(dcbpy)_2dppz]^{2+}$ in DNA duplex of DNA NFs.

## 2. Experimental Section

### 2.1 Target Transduction and Amplification Procedure

As seen in Scheme 1B, the target-recycling magnification procedure based on DSN enzyme was employed. In detail, 100 mL of magnetic bead (5 mg/mL) was diluted with 900 μL of PBS (0.1 M). Next, EDC (20 μL, 0.2 M) and NHS (20 μL, 0.2 M) was added into the above mixture to activate the carboxyl on MBD (magnetic bead), followed by adding Hairpin DNA (20 μL, 100 μM). For coupling with MBD, the mixture was stirred for 12 h at 4 ℃. After that, 10 μL of HT (hexanethiol) (1 mM) was applied to block the nonspecific sites. With the addition of DSN enzyme, 1×DSN master buffer and target microRNA-141, the mixture solution was incubating at 65 ℃ for 40 min. The hairpin DNA was opened by target microRNA-141 and a DNA-RNA duplex was generated. According to the literatures, DSN enzyme possesses high selectivity for cleaving DNA in DNA-RNA duplex (≥15 base pairs) and DNA duplex

(≥10 base pairs), while displays tiny ability for cleaving single-stranded DNA, RNA duplex and single-stranded RNA.[33,34] Therefore, the DNA-RNA duplex was cleaved by DSN enzyme with releasing product DNA and reusing target microRNA-141. Then, 2 μL of DSN stop solution was added into the mixture solution to denature the DSN enzyme for 10 min. Finally, the magnet was employed to separate the mixture solution to obtain the product DNA, which could act as the initiator of the RCR reaction.

### 2.2 Preparation of DNA NFs

RCR reaction was executed with mixing primer DNA (2.5 μM), circular DNA template (1:1) (*V:V*), 2.5 μL 1×phi29 polymerase buffer, 0.5 μL phi29 polymerase, and 2.5 μL dNTPs for 4 h at 37 °C.

### 2.3 Fabrication Process of the Sensing Interface

First, the bare GCE was pretreated using alumina powder followed by ultrasonicating it before modification using ultrapure water. Next, PTB7-Th solution dissolved in tolune was immobilized on the bare GCE. Subsequently, to deposit gold nanoparticles (Au NPs) on the modified electrode, the decorated electrode was submerged in gold chloride tetrahydrate ($HAuCl_4$) (1%) solution with -0.2 V. Then, 20 μL of linker DNA (2.5 μM) was decorated on the resultant electrode at 4 ℃ for 12 h. Finally, to block nonspecific binding sites, 20 μL of HT solution (1 mM) was added on the modified electrode for 40 min at room temperature. The sensing interface was fabricated and then the decorated electrode was washed to eliminate the redundant reagents by distilled water after each decoration. The fabricated process of the PEC biosensor was detailedly described in Scheme 1.

### 2.4 PEC Biosensor Measurement

PEC biosensor measurement was tested in PBS (6 ~ 8 mL, pH 7.0, 0.1 M) without any addition of electronic donor or acceptor at room temperature. The light emitting diode lamp acted as excitation light source in our measurement system with the wavelength of 623 nm, which possess a luminous flux of 31 mW and turn off-on-off for 10-20-10 s with 0.0 V.

## 3. Results and discussion

### 3.1 Characterization of the Synthesized Materials

The morphology of the materials was characterized by scanning electron microscope (SEM). The SEM images of nano-$C_{60}$ was putted in Supplementary Material (Figure S5). Figure 1A is the SEM image of PTB7-Th. And Figure 1B shown the SEM image of electrochemically deposited Au NPs on PTB7-Th/GCE. In this image, a large surface of PTB7-Th on GCE and a large amount of Au NPs on the surface of PTB7-Th could be observed, which proved the successful deposition of Au NPs on PTB7-Th. Fluorescence emission and excitation spectrums and ultraviolet-visible (UV-vis) absorption spectrums were applied to further verifying the successful preparation of PTB7-Th. As seen in Figure 1C, in the presence of PTB7-Th, two broad emission peaks at 643 nm and 734 nm were observed with excitation wavelength at 570 nm within the emission wavelength range of 600 nm to 790 nm, which belongs to the characteristic fluorescence emission peaks of PTB7-Th. Meanwhile, the characteristic fluorescence excitation peak of PTB7-Th at 567 nm was obtained with emission wavelength at 643 nm within the excitation wavelength range of 400 nm to 680 nm upon the addition of PTB7-Th. Furthermore, the UV-vis absorption spectroscopy of PTB7-Th was shown in Figure 1D, the characteristic

absorption peaks of PTB7-Th were observed around 248 nm, 318 nm, 633 nm and 697 nm, and consistent with the previous literature in the UV-vis region (200 nm < λ < 800 nm).[23] All the results verified the successful preparation of material.

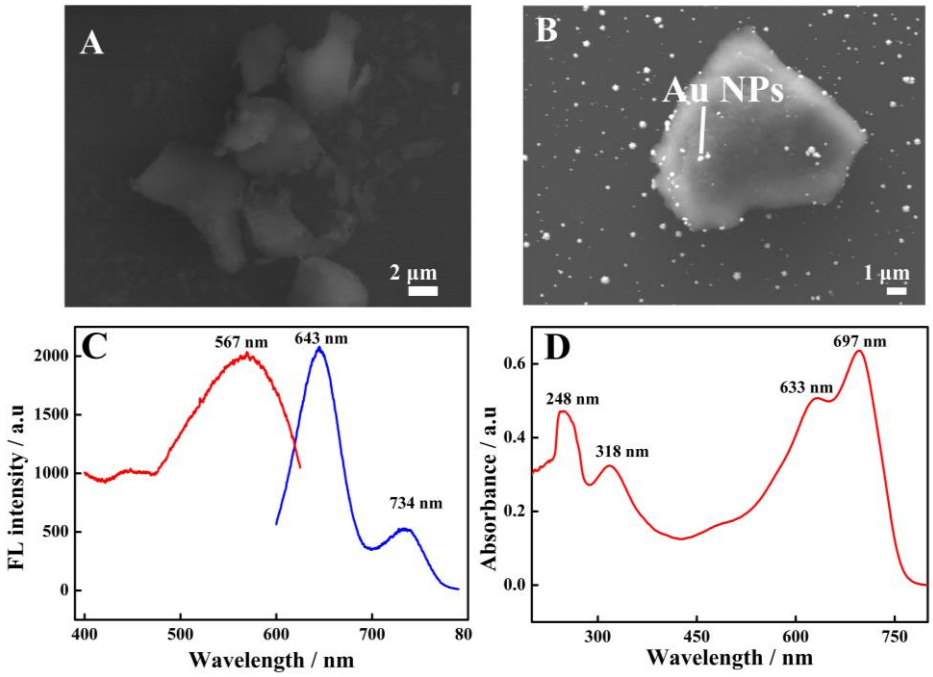


**Figure 1.** (A) The SEM image of PTB7-Th; (B) The SEM image of PTB7-Th deposited Au NPs; (C) Fluorescence emission spectrums of PTB7-Th with excitation at 570 nm within the emission wavelength range of 600 nm to 790 nm; Fluorescence excitation spectrums of PTB7-Th with emission at 643 nm within the excitation wavelength range of 400 nm to 680 nm; (D) UV-vis adsorption spectrum of PTB7-Th.

### 3.2 Signal Comparison of Electrode Incubated with Different Materials

To illustrate the superiority of $[Ru(dcbpy)_2dppz]^{2+}$ and nano-$C_{60}$ as the sensitizers of PTB7-Th, comparison experiments were implemented by incubating different materials on the electrode including (A) PTB7-Th (D-A-type photoactive material), (B) nano-$C_{60}$ (immobilized on DNA NFs surface) and PTB7-Th, (C) $[Ru(dcbpy)_2dppz]^{2+}$ (sensitizer, embedded in DNA duplex grooves of DNA NFs) and PTB7-Th, (D) nano-$C_{60}$ (sensitizer, immobilized on DNA NFs surface),

10.1002/chem.201806005

$[Ru(dcbpy)_2dppz]^{2+}$ (sensitizer, embedded into DNA duplex grooves of DNA NFs) and PTB7-Th. The photocurrent responses for different materials were shown in Figure 2. As shown in Figure 2A, after immobilizing donor-acceptor-type photoactive material (PTB7-Th) on bare GCE, about 258 nA photocurrent response was obtained. In Figure 2B, 830 nA photocurrent response was observed by immobilizing nano-$C_{60}$ on the surface of DNA NFs without $[Ru(dcbpy)_2dppz]^{2+}$. After embedding $[Ru(dcbpy)_2dppz]^{2+}$ in the DNA duplex grooves of DNA NFs without nano-$C_{60}$, an evidently improved photocurrent signal (1424 nA) could be observed in Figure 2C, which was 6 times greater than that of PTB7-Th photocurrent response. A further enhanced photocurrent signal (1770 nA) was observed by simultaneously embedding $[Ru(dcbpy)_2dppz]^{2+}$ in the grooves of DNA duplex and immobilizing nano-$C_{60}$ on the surface of DNA NFs in Figure 2D, which is close to 7 times greater than that of PTB7-Th. The comparison results clearly indicated that the sensitizers ($[Ru(dcbpy)_2dppz]^{2+}$ and nano-$C_{60}$) could obviously enhance the PCE of PTB7-Th, leading to the possibility for co-sensitization of PTB7-Th and photocurrent response amplification for the proposed biosensor.

10.1002/chem.201806005

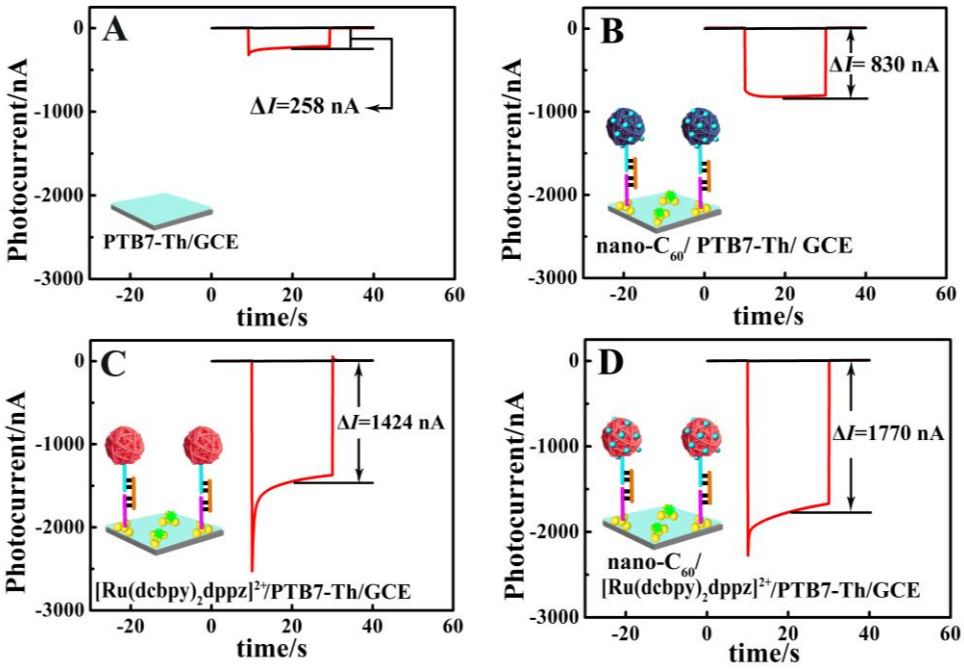


**Figure 2**. Different photocurrent responses of biosensor decorated with different materials: (A) PTB7-Th material; (B) nano-$C_{60}$ (sensitizer, immobilized on DNA NFs surface) and PTB7-Th; (C) $[Ru(dcbpy)_2dppz]^{2+}$ (sensitizer, embedded in the grooves of DNA duplex) and PTB7-Th; (D) nano-$C_{60}$ (sensitizer, immobilized on DNA NFs surface), $[Ru(dcbpy)_2dppz]^{2+}$ (sensitizer, embedded in the grooves of DNA duplex) and PTB7-Th.

### 3.3 The Analytical Performance of the Proposed Biosensor

The analytical performance of the proposed biosensor was assessed by detecting various concentrations of microRNA-141 using the proposed platform. As shown in Figure 3A, with the increasing of target concentration, the photocurrent response increased linearly, showing a nice linear relationship between the corresponding photocurrent response and the logarithm of the microRNA-141 concentration from 2.5 fM to 2.5 nM in Figure 3B. The estimated limit of detection (LOD) and limit of quantification (LOQ) were down to 0.83 fM and 2.77 fM, respectively. The linear regression equation was $I$ = -500.4 - 205.1 lg $c_{target}$, with a correlation coefficient of 0.9939. Here, $c_{target}$ and $I$ presented the concentration of microRNA-141 and

photocurrent response, respectively. The analytical performance of the proposal method was compared with previous study for detection of microRNA. As seen in Table 1, the proposed PEC strategy displayed a much wider linear range and a highly sensitivity, which might be attributed to the significantly enhanced photocurrent of the proposed strategy.

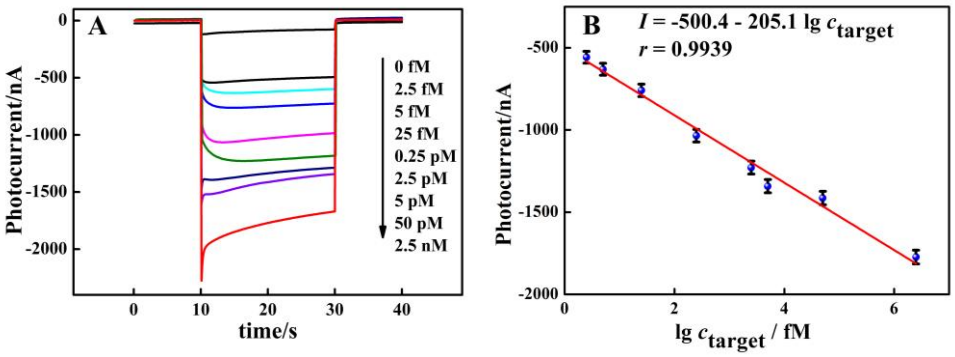


**Figure 3.** (A) The photocurrent responses of the proposed strategy with various concentrations microRNA-141 (2.5 nM, 50 pM, 5 pM, 2.5 pM, 0.25 pM, 25 fM, 5 fM, 2.5 fM, 0 fM), (B) Calibration curve of the proposed strategy toward microRNA-141 standards with various concentrations (2.5 nM, 50 pM, 5 pM, 2.5 pM, 0.25 pM, 25 fM, 5 fM, 2.5 fM).

**Table 1** Comparison of the Presented Strategies with Reported works.

| Detection method | Linear range | LOD | Ref. |
|---|---|---|---|
| fluorescent assay | 0.1 nM ~ 8 μM | 0.06 nM | 35 |
| DPV | 20 fM ~ 50 pM | 5.36 fM | 36 |
| fluorescent assay | 5 nM ~ 1000 nM | 5 nM | 37 |
| EIS | 2.0 fM ~ 2.0 pM | 1.0 fM | 38 |
| chemiluminescence | 20 fM ~ 5.0 pM | 10 fM | 39 |
| fluorescent assay | 3.8 pM ~ 10 nM | 3.8 pM | 40 |
| PEC | 350 fM ~ 5 nM | 153 fM | 41 |
| PEC | 2.5 fM ~ 2.5 nM | 0.83 fM | ***Our work*** |

**Abbreviations:** electrochemical impedance spectroscopic (EIS); differential pulse voltammetry (DPV).

### 3.4 PEC Mechanism of the Biosensor

10.1002/chem.201806005

The PEC mechanism of the biosensor was illustrated in Figure 4. For the purpose of ultrasensitive detection, high photocurrent response and low electron-hole recombination are necessary for PEC biosensor. Nano-$C_{60}$ as a classic photosensitive material, possesses strong electron-accepting ability and high PCE. But its applications were limited by its wide band gap ($E_g$ = 2.6 eV).[42] Therefore, using a narrow-band gap material to modify nano-$C_{60}$ to obtain a sensitized structure is desirable. $[Ru(dcbpy)_2dppz]^{2+}$ as a traditional photosensitive material, the computed energy band gap is 2.36 eV (the computational process was showed in Supplementary Material), which is lower than that of nano-$C_{60}$. Furthermore, PTB7-Th is a donor-acceptor-type photoactive material, which possesses a much lower energy band gap ($E_g$ = 1.58 eV) than that of $[Ru(dcbpy)_2dppz]^{2+}$. As can be seen, the energy band gaps matched well between PTB7-Th, $[Ru(dcbpy)_2dppz]^{2+}$ and nano-$C_{60}$. In our strategy, coupling the three photosensitive materials could obviously enhance the PCE and increase the energy utilization efficiency of PTB7-Th, it was an ideal strategy to achieve photocurrent amplification of the proposed biosensor and ultrasensitive detection of microRNA-141.

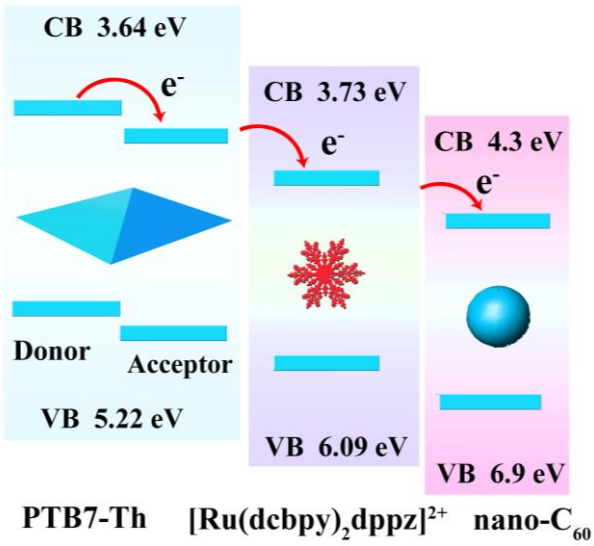

**Figure 4.** Schematic explaination of electron-transfer mechanism of PTB7-Th/ $[Ru(dcbpy)_2dppz]^{2+}$/ nano-$C_{60}$ photosensitive materials (CB: conductive band; VB: valence band).

### 3.5 Stability and Selectivity of the Biosensor

To investigate the selectivity of the presented biosensor, microRNA-155, microRNA-21, let-7a and thrombin (TB) were chosen as interferences and microRNA-141was chosen as a target model. In Figure 5A, no obvious photocurrent signal of the microRNA-155, microRNA-21, let-7a and TB (the concentrations of each interferences were 2 nM) could be obtained except the target microRNA-141 (0.25 nM). The comparison results demonstrated the superior selectivity, which generated from the specific cleavage for DNA double-strand and DNA in DNA-RNA hetero-duplex of DSN in the proposed PEC strategy. Meanwhile, the stability was evaluated through continuous measuring using 2.5 pM of microRNA-141 as target. The proposed biosensor showed a good stability with the relative standard deviation (RSD) of 1.41% by continuous scanning for 11 circles in Figure 5B. The result suggested good stability for the established biosensor.

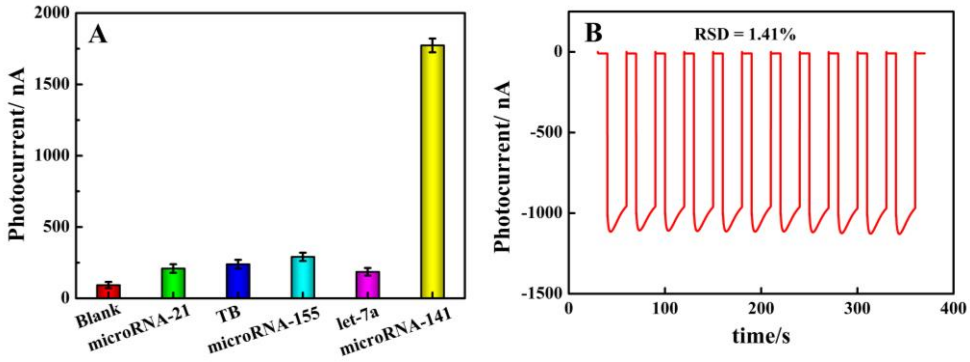


**Figure 5.** (A) The photocurrent of the proposed biosensor incubated with interferences: TB (2 nM), microRNA-21 (2 nM), microRNA-155 (2 nM), let 7a (2 nM), target microRNA-141 (0.25 nM) and blank; (B) Stability of the established strategy in the presence of microRNA-141 (2.5 pM).

### 3.6 Evaluation of the Proposed Biosensor Applicability for MicroRNA with different Cancer Cells

A recovery experiment was performed using five kinds of cancer cells as real samples to assess the actual applicability of the proposed strategy. It is well-known that MB231, 22Rv1, A549, MCF-7 and Hela were five representative human cancer cells with different expression levels of microRNA-141. As shown in Figure 6, with the increasing numbers of MB231 and 22Rv1 cells in total RNA extraction solutions from 10 to 5000, a significantly enhanced photocurrent response of the proposed PEC biosensor could be obtained. Concretely, the photocurrent signal intensities displayed in Figure 6A and 6B corresponding to the microRNA-141 expression levels in MB231 and 22Rv1 cell, respectively. Meanwhile, as shown in Figure 6C, the PEC signal of Hela, A549 and MCF-7 cells obviously decreased compared with MB231 and 22Rv1 cells, which demonstrated the microRNA-141 has a higher expression level in MB231 and 22Rv1 cells and a lower expression level in Hela, A549 and MCF-7 cells. The concentration of microRNA-141 showed in above results was consistent with literatures.[33,43] The results represented the good potential application of the established strategy for microRNA detection with good selectivity, high sensitivity and accuracy, which was significant for biomarker analysis and cancer diagnosis.

10.1002/chem.201806005

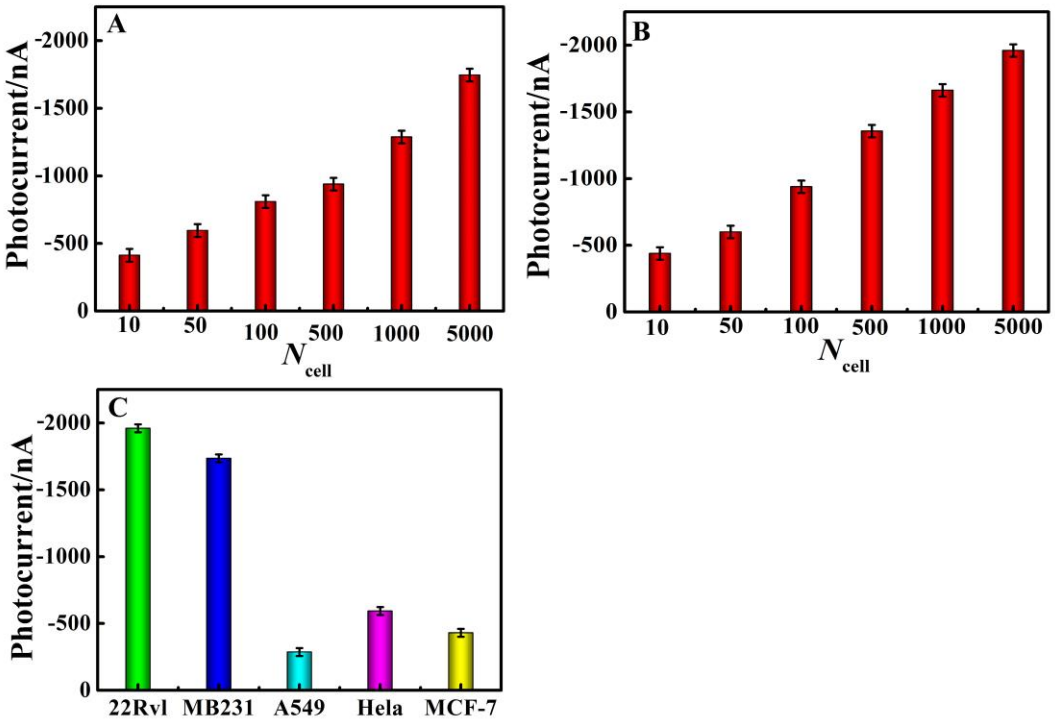


**Figure 6.** (A) Photocurrent signals of the proposed biosensor in the presence of different numbers of MB231 cancer cells; (B) Photocurrent signals of the proposed biosensor in the presence of different numbers of 22Rv1 cancer cells; (C) Photocurrent signals of the proposed PEC biosensor in the presence of five different cancer cells (22Rv1, MB231, A549, HeLa and MCF-7 cancer cells).

## 4. Conclusions

In summary, an ultrasensitive PEC strategy was established using photoactive material (PTB7-Th) as a signal indicator, which was co-sensitized by $[Ru(dcbpy)_2dppz]^{2+}$ and nano-$C_{60}$ for microRNA assay with the assistance of DSN assisted target-recycling magnification technique. In this work, the proposed strategy provided a new method to numerously and simultaneously immobilize two types of sensitizers on the surface of photoactive material. Meanwhile, the PCE of the photoactive material (PTB7-Th) was significantly improved by embedding $[Ru(dcbpy)_2dppz]^{2+}$ in DNA duplex and immobilizing nano-$C_{60}$ on the surface of

DNA NFs, leading to the signal enhancement of the proposed PEC strategy. Compared with conventional PEC assay, this PEC biosensor showed lower background signal, higher PCE and significantly enhanced photocurrent response. Furthermore, the proposed PEC biosensor showed wide linear range, excellent selectivity and good sensitivity for assay of microRNA, exhibited great potential in PEC assay and offered a new approach for early diagnosis of cancer.

## Acknowledgements

This work was financially supported by the Fundamental Research Funds for the Central Universities (Grants XDJK2017A001), and the China National Natural Science Foundation (NNSF) of China (Grants 21775124， 21675129, 21575116, and 51473136).

## References

[1]. R. Gill, M. Zayats, I. Willner, S Angew. Chem., Int. Ed. 2008, 47, 7602-7625.

[2]. L. Li, , Y. Zhang, L. N. Zhang, S. G. Ge, H. Y. Liu, N. Ren, M. Yan, J. H. Yu, Anal. Chem. 2016, 88 5369-5377.

[3]. W. W. Zhao, J. J. Xu, H. Y. Chen, Chem. Soc. Rev. 2015, 44, 729-741.

[4]. Y. C. Zhu, N. Zhang, Y. F. Ruan, W. W. Zhao, J. J. Xu, H. Y. Chen, Anal. Chem. 2016, 88, 5626-5630.

[5]. J. Tang, J. Li, P. Da, Y. Wang, G. Zheng, Chem. Eur. J. 2015, 21, 11288 – 11299.

[6]. Q. Wan, X. Guo, Z. Wang, W. Li ,B. Guo, W. Ma, M. Zhang, Y. Li, Adv. Funct. Mater. 2016, 26, 6635–6640.

[7]. L. Lu, W. Chen, T. Xu, L. Yu, Nat. Commun. 2015, 6, 7327-7334.

[8]. J. Gao, W. Wang, C. Zhan, Y. Hu, S. Xiao, X. Lu, W. You, J. Mater. Chem. A,

2018, 6, 20788–20794

[9]. Y. N. Zheng, W. B. Liang, C. Y. Xiong, Y. L. Yuan, Y. Q. Chai, R. Yuan, Anal. Chem. 2016, 88, 8698-8705.

[10]. Y. H. Zhang, Y. N. Zheng, M. J. Li, T. Hu, R. Yuan, S. P. Wei, Anal. Chem. 2018, 90, 12278−12283

[11]. G. G. Frank, J. B. Allen, J. Am. Chem. Soc. 2000, 122, 7426-7427.

[12]. H. Rudmann, S. Shimada, M. S. Rubner, J. Am. Chem. Soc. 2002, 124, 4918-4921.

[13]. C. Y. Chen, S. J. Wu, C. G. Wu, C. G. Chen, K. C. Ho, Angew. Chem. 2006, 118, 5954-5957.

[14]. T. Kono, N. Masaki, M. Nishikawa, R. Tamura, H. Matsuzaki, M. Kimura, S. Mori, Appl. Mater. Interfaces 2016, 8, 16677-16683.

[15]. K. Kalyanasundaram, J. Kiwi, M. Grätzel, Helv. Chim. Acta. 1978, 61, 2720-2730.

[16]. A. Juris, V. Balzani, F. Barigelletti, S. Campagna, P. Belser, A. V. Zelewsky, Chem. Rev. 1988, 84, 85-277.

[17]. C. M. Dupureur, J. K. Barton, J. Am. Chem. Soc. 1994, 116, 10286-10287.

[18]. A. E. Friedman, J. C. Chambron, J. P. Sauvage, N. J. Turro, J. K. Barton, J. Am. Chem. Soc. 1990, 112, 4960-4962.

[19]. C. J. Murphy, M. R. Arkin, N. D. Ghatlia, Proc. Natl. Acad. Sci. 1994, 91, 5315-5319.

[20]. C. Turro, S. H. Bossmann, Y. Jenkins, J. K. Barton, N. J. Turro, J. Am. Chem. Soc. 1995, 117, 9026-9032.

[21]. M. Buhl, A. Hirsch, Chem. Rev., 2001, 101, 1153-1183.

[22]. D. M. Guldi, G. M. Aminur Rahman, V. Sgobba, C. Ehli, Chem. Soc. Rev. 2006, 35, 471-487.

[23]. S. H. Liao, H. J. Jhuo, Y. S. Cheng, S. A. Chen, Adv. Mater. 2013, 25, 4766-4771.

[24]. Y. Liang, Z. Xu, J. Xia, S. T. Tsai, Y. Wu, G. Li, C. Ray, L. Yu, Adv. Mater. 2010, 22, 135-138.

[25]. J. Sukegawa, C. Schubert, X. Z. Zhu, H. Tsuji, D. M. Guldi, E. Nakamura, Nat. Chem. 2014, 6, 899-905.

[26]. R. Hu, X. B. Zhang, Z. L. Zhao, G. Z. Zhu, T. Chen, T. Fu, W. H. Tan, Angew. Chem. 2014,126, 5931-5936.

[27]. G. Z. Zhu, R. Hu, Z. L. Zhao, Z. Chen, X. B. Zhang, W. H. Tan, J. Am. Chem. Soc. 2013, 135, 16438-16445.

[28]. N. Hao, P. P. Dai, T. Yu, J. J. Xu, H. Y. Chen, Chem. Commun. 2015, 51, 13504-13507.

[29]. J. B. Lee, J. Hong, D. K. Bonner, Z. Poon, P. T. Hammond, Nat. Mater. 2012, 11, 316-322.

[30]. Y. F. Lv, R. Hu, G. Z. Zhu, X. B. Zhang, L. Mei, Q. L. Liu, L. P. Qiu, C. C. Wu, W. H. Tan, Nat Protoc. 2015, 10, 1508–1524.

[31]. S. K. Li, A. Y. Chen, X. X. Niu, Z. T. Liu, M. Du, Y. Q. Chai, R. Yuan, Y. Zhuo, Chem. Commun., 2017, 53, 9624-9627.

[32]. L. Shi, C. L. Mu, T. Gao, T. S. Chen, S. Hei, J. Yang, G. X. Li, Chem. Commun., 2018, 54, 11391-11394.

[33]. F. Degliangeli, P. Kshirsagar, V. Brunetti, P. P. Pompa, R. Fiammengo, J. Am. Chem. Soc. 2014, 136, 2264-2267.

[34]. F. Ma, W. J. Liu, Q. Y. Zhang, C. Y. Zhang, Chem. Commun., 2017, 53, 10596-10599.

[35]. S. S. Lu, S. Wang, J. H. Zhao, J. Sun, X. R. Yang, Anal. Chem. 2017, 89, 8429-8436.

[36]. Y. Y. Yu, Z. G. Chen, L. J. Shi, F. Yang, J. B. Pan, B. B. Zhang, D. P. Sun, Anal. Chem. 2014, 86, 8200-8205.

[37]. R. Liao, K. He, C. Y. Chen, X. M. Chen, C. Q. Cai, Anal. Chem. 2016, 88, 4254-4258.

[38]. Y. Q. Ren, H. M. Deng, W. Shen, Z. Q. Gao, Anal. Chem. 2013, 85, 4784-4789.

[39]. H. M. Deng, Y. Q. Ren, W. Shen, Z. Q. Gao, Chem. Commun. 2013, 49, 9401-9403.

[40]. W. Wang, T. Kong, D. Zhang, J. N. Zhang, G. S. Cheng, Anal. Chem. 2015, 87, 10822-10829.

[41]. W. W. Tu, H. J. Cao, L. Zhang, J. C. Bao, X. H. Liu, Z. H. Dai, Anal. Chem. 2016, 88, 10459-10465.

[42]. K. Kim, T. H. Lee, E. J. G. Santos, P. S. Jo, A. Salleo, Y. Nishi, Z. N. Bao, ACS Nano 2015, 9, 5922-5928.

[43]. B. C. Yin, Y. Q. Liu, B. C. Ye, J. Am. Chem. Soc. 2012, 134, 5064-5067.

10.1002/chem.201806005

For TOC only